The α2δ-1–NMDA receptor coupling is essential for corticostriatal long-term potentiation and is involved in learning and memory

Received for publication, May 15, 2018, and in revised form, October 18, 2018 Published, Papers in Press, October 24, 2018, DOI 10.1074/jbc.RA118.003977

Jing-Jing Zhou[‡], De-Pei Li[‡], Shao-Rui Chen[‡], Yi Luo[‡§], and Hui-Lin Pan[‡1]

From the [‡]Center for Neuroscience and Pain Research, Department of Anesthesiology and Perioperative Medicine, University of Texas M. D. Anderson Cancer Center, Houston, Texas 77030 and the [§]Department of Clinical Laboratory Medicine, Zhongnan Hospital of Wuhan University, Wuhan, Hubei 430071, China

Edited by Mike Shipston

The striatum receives extensive cortical input and plays a prominent role in motor learning and habit formation. Glutamate *N*-methyl-D-aspartate (NMDA) receptor (NMDAR)-mediated long-term potentiation (LTP) is a major synaptic plasticity involved in learning and memory. However, the molecular mechanism underlying NMDAR plasticity in corticostriatal LTP is unclear. Here, we show that theta-burst stimulation (TBS) consistently induced corticostriatal LTP and increased the coincident presynaptic and postsynaptic NMDAR activity of medium spiny neurons. We also found that α2δ-1 (previously known as a subunit of voltage-gated calcium channels; encoded by the *Cacna2d1* gene) physically interacted with NMDARs in the striatum of mice and humans, indicating that this cross-talk is conserved across species. Strikingly, inhibiting α2δ-1 trafficking with gabapentin or disrupting the α2δ-1–NMDAR interaction with an α2δ-1 C terminus–interfering peptide abolished TBS-induced LTP. In *Cacna2d1*-knockout mice, TBS failed to induce corticostriatal LTP and the associated increases in presynaptic and postsynaptic NMDAR activities. Moreover, systemic gabapentin treatment, microinjection of α2δ-1 C terminus–interfering peptide into the dorsomedial striatum, or *Cacna2d1* ablation impaired the alternation T-maze task and rotarod performance in mice. Our findings indicate that the interaction between α2δ-1 and NMDARs is of high physiological relevance and that a TBS-induced switch from α2δ-1–free to α2δ-1–bound NMDARs is critically involved in corticostriatal LTP and LTP-associated learning and memory. Gabapentinoids at high doses may adversely affect cognitive function by targeting α2δ-1–NMDAR complexes.

Learning and memory crucially depend on long-lasting synaptic plasticity in neuronal networks including the hippocampus, cortex, and striatum. The striatum, the largest part of the forebrain input regions, plays critical roles in skill development, instrumental learning, and habit formation (1–3). The long-term potentiation (LTP)[2] at corticostriatal synapses may constitute cellular substrates of learning and memory (4–7). The glutamate NMDARs are essential for the synaptic plasticity that underlies LTP induction in the striatum (7, 8). The medium spiny neurons (MSNs) in the striatum are GABAergic inhibitory cells, which receive extensive cortical glutamatergic input and projects to the output structures of the basal ganglia (9, 10). Cortical input to MSNs in the striatum is involved in the early formation of working memory, which critically depends on synaptic NMDARs (11–13). However, the molecular mechanism responsible for changes in synaptic NMDAR activity during corticostriatal LTP induction remains poorly understood.

α2δ-1, encoded by *Cacna2d1*, is commonly known as a subunit of voltage-gated calcium channels (VGCCs) (14). For a long time, α2δ-1 has been considered to be engaged exclusively in the regulation of VGCCs. However, α2δ-1 has a weak interaction with VGCC α1 subunits in the brain (15), and VGCC currents in brain neurons are similar in WT and *Cacna2d1*-knockout mice (16). In addition, the α2δ-1–binding drug gabapentin does not affect VGCC activity, the interaction between Cavα1 and α2δ-1, or VGCC-dependent neurotransmitter release (17–20). α2δ-1 is mainly present at the excitatory synapses throughout the mammalian brain (21, 22). We recently discovered that α2δ-1 physically interacts with NMDARs in the spinal cord to promote neuropathic pain development (17). Interestingly, γ2 (stargazin) was also identified initially as a VGCC subunit but is now known to play primary roles in regulating AMPA receptors (23). Although α2δ-1 is involved in neurological disorders including epilepsy and chronic pain, its physiological role in learning and memory remains unknown. Because α2δ-1 is highly expressed in the cortical and striatal regions (21, 22), we determined whether α2δ-1–bound NMDARs are involved in corticostriatal LTP induction. We present our new findings that α2δ-1 is essential for corticostriatal LTP and the associated increase in the presynaptic and post-

This work was supported by the National Institutes of Health Grants GM120844 and NS101880 (to H.-L. P.) and by the N. G. and Helen T. Hawkins Endowment. The authors declare that they have no conflicts of interest with the contents of this article. The content is solely the responsibility of the authors and does not necessarily represent the official views of the National Institutes of Health.

[1] To whom correspondence should be addressed: Dept. of Anesthesiology and Perioperative Medicine, Unit 110, University of Texas M. D. Anderson Cancer Center, 1515 Holcombe Blvd., Houston, TX 77030. Tel.: 713-563-5838; Fax: 713-794-4590; E-mail: huilinpan@mdanderson.org.

[2] The abbreviations used are: LTP, long-term potentiation; NMDA, *N*-methyl-D-aspartate; NMDAR, NMDA receptor; TBS, theta-burst stimulation; MSN, medium spiny neuron; VGCC, voltage-gated calcium channel; EPSP, excitatory postsynaptic potential; AP5, (2*R*)-amino-5-phosphonopentanoate; IP, immunoprecipitation; mEPSC, miniature excitatory postsynaptic current; ANOVA, analysis of variance.

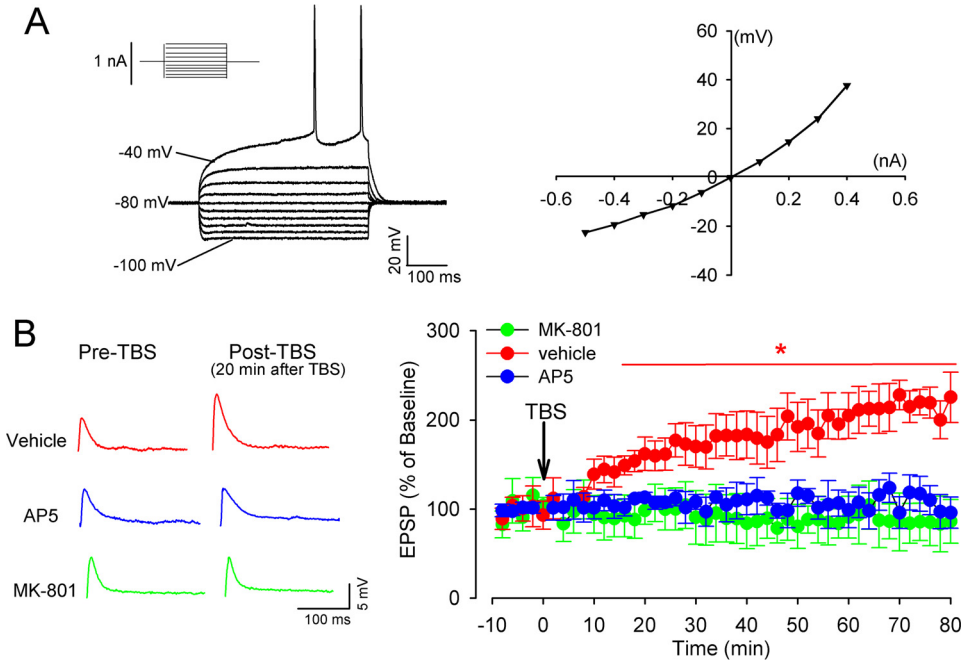

Figure 1. Synaptic NMDARs are essential for TBS-induced LTP in MSNs in the dorsomedial striatum. *A*, representative current-clamp recording of an MSN in response to current steps (*left panel*) and the current-voltage plot of the same neuron (*right panel*). Inward rectification and long latency to first spike were used to identify the MSN. *B*, representative original traces (20 min after TBS) and time course of changes of EPSPs in response to TBS in MSNs recorded in the presence of vehicle, 50 μM AP5, or MK-801 contained in the recording pipette solution ($n = 15$ neurons in each group). The data are means ± S.E. *, $p < 0.05$ (*versus* baseline). One-way repeated measures of ANOVA followed by Dunnett's post hoc test.

synaptic NMDAR activity of MSNs in the dorsomedial striatum. We also show the important role of α2δ-1–NMDAR complexes in the physiological process such as striatal learning and memory. This information advances our understanding of the molecular mechanisms that govern the synaptic plasticity engaged in learning and memory.

Results

Theta-burst stimulation induces corticostriatal LTP through synaptic NMDARs

Theta-burst stimulation (TBS) can mimic the theta rhythm firing of dorsomedial neurons during various cognitive tasks (24, 25). In extracellular recording of population spikes, TBS is much more effective than is single tetanic stimulation at evoking LTP in the dorsomedial striatum (8). MSNs constitute the major cell type, comprising ~95% of striatal neurons in rodents (26). We performed whole-cell recording of excitatory postsynaptic potentials (EPSPs) in individual MSNs to determine the TBS-induced LTP in the dorsomedial striatum of mice. The MSNs were visually identified in brain slices and were characterized by inward rectification and delayed firing in response to depolarization (Fig. 1*A*), as reported previously (27, 28). As expected, TBS (10 trains of stimuli spaced at 10-s intervals, with each train containing bursts of 4 spikes at 100 Hz, repeated 10 times at 5 Hz) (8) in cortical layer VI reliably induced a profound increase in the amplitude of EPSPs in all MSNs after a latency of ~10 min; this increase lasted for at least 80 min (Fig. 1). The time course of this electrical TBS-induced LTP expression (via whole-cell current-clamp recording in parasagittal striatal slices) was similar to what was induced using an optical TBS approach (7).

To determine whether NMDARs are required for TBS-induced corticostriatal LTP in MSNs, we performed an EPSP recording in the presence of (2*R*)-amino-5-phosphonopentanoate (AP5, 50 μM), a specific NMDAR antagonist. Treatment with AP5 abolished LTP induction by TBS in all recorded MSNs (Fig. 1*B*).

Presynaptic NMDARs at cortical axon terminals are critically involved in TBS-induced corticostriatal LTP (7). We next determined whether postsynaptic NMDARs are similarly involved in corticostriatal LTP induced by TBS. We blocked the postsynaptic NMDARs of MSNs through intracellular dialysis of MK-801 (50 μM), an NMDAR open-channel blocker, included in the pipette recording solution (29). TBS failed to induce LTP in all MSNs when an MK-801–containing intracellular solution was used for whole-cell recording (Fig. 1*B*). Thus, both presynaptic and postsynaptic NMDARs are equally important to corticostriatal LTP induction.

α2δ-1 physically interacts with NMDARs in the striatum

We recently showed that α2δ-1 is a new interacting protein of NMDARs in the spinal cord and potentiates synaptic NMDAR activity (17). α2δ-1 is abundantly expressed in excitatory synapses in various brain regions (21). Because GluN1 is an obligatory subunit of NMDARs, we determined whether α2δ-1 physically interacts with GluN1 in the striatum. Co-immunoprecipitation (co-IP) assays showed that α2δ-1 antibody, not the irrelevant IgG, precipitated the GluN1 protein in both the mouse (Fig. 2*A*) and human striatal tissues (Fig. 2*B*). Furthermore, immunoblotting using the flow-through samples (*i.e.* removing the α2δ-1–bound GluN1 protein complex; Fig. 2*C*) showed that α2δ-1–free GluN1 protein bands were still

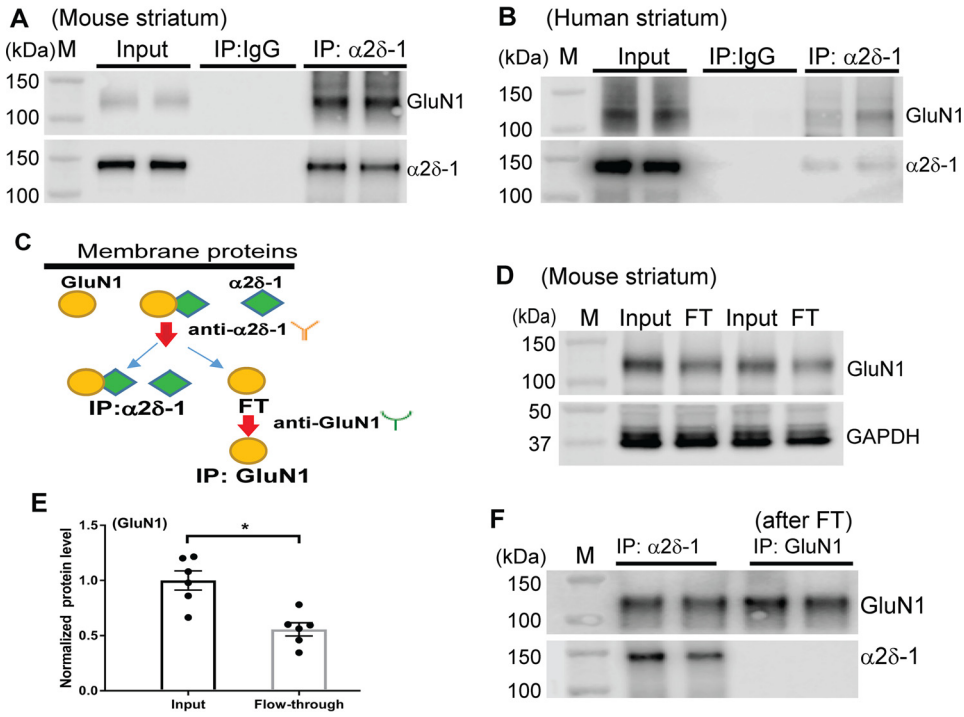

Figure 2. α2δ-1 physically interacts with GluN1 in the striatum of mice and humans. *A* and *B*, co-IP analysis shows the protein–protein interaction between α2δ-1 and GluN1 in the membrane extracts from striatal tissues of mice (*A*) and humans (*B*, two separate subjects). The proteins were immunoprecipitated initially with a mouse anti–α2δ-1 antibody or IgG. Western immunoblotting was performed using a rabbit anti-GluN1 or a rabbit anti–α2δ-1 antibody. IgG and input (tissue lysates only, without immunoprecipitation) were used as negative and positive controls. Similar data were obtained from striatal tissues from each of the four human donors. *C*, a schematic shows the determination of relative amounts of GluN1 proteins in the membrane fraction of the mouse striatum using a two-step co-IP protocol. *D* and *E*, representative gel images (two pairs of samples) and quantification show the relative amount of GluN1 proteins present in the input (total membrane protein lysates) and flow-through (*FT*) samples from mouse striatal tissues ($n = 6$ samples/group). *F*, original gel images show that both GluN1 and α2δ-1 were present in samples pulled down by α2δ-1 antibody. However, GluN1, but not α2δ-1, was detected in FT samples subjected to immunoprecipitation using GluN1 antibody (shown in *C*). *M*, molecular marker. *, $p < 0.05$ (*versus* input). Paired Student's *t* test was used.

detected (Fig. 2*D*). Compared with the input samples (total membrane protein lysates), a considerable portion (55.7%) of membrane GluN1 proteins was not bound to α2δ-1 (Fig. 2*E*). Immunoblotting of flow-through samples that were subjected to further immunoprecipitation using GluN1 antibody showed that only GluN1, but not α2δ-1, was detected, confirming that GluN1 is not bound to α2δ-1 in flow-through samples (Fig. 2*F*). These results suggest that ~44.3% of membrane NMDARs form a protein complex with α2δ-1 in the striatum.

α2δ-1 is critically required for TBS-induced corticostriatal LTP

Although NMDARs are relatively stable at the synaptic site (30), many synaptic NMDARs are also quite mobile and dynamic at synaptic sites (31, 32). Because α2δ-1 promotes NMDAR surface expression and synaptic targeting (17), we determined whether α2δ-1–bound NMDARs are involved in TBS-induced corticostriatal LTP. Gabapentin is an inhibitory α2δ-1 ligand (33, 34) and is used clinically to treat patients with neuropathic pain and epilepsy. Gabapentin predominantly inhibits the synaptic/surface trafficking of α2δ-1–bound NMDARs (17). The mouse brain slices were pretreated with gabapentin (100 μM) for 30–60 min before LTP induction. In brain slices treated with gabapentin, TBS did not increase the amplitude of EPSPs in any of the MSNs examined (Fig. 3*A*).

α2δ-1 interacts with NMDARs predominantly through its transmembrane C terminus (17). We used a 30-amino acid peptide (VSGLNPSLWSIFGLQFILLWLVSGSRHYLW) mimicking the C-terminal domain of α2δ-1, which specifically diminishes the α2δ-1–NMDAR interaction (17). Because α2δ-1 primarily promotes forward trafficking of intracellular α2δ-1–bound NMDARs, we fused the peptide to the cell-penetrating peptide Tat (YGRKKRRQRRR), generating α2δ-1Tat peptide to disrupt the interaction between α2δ-1 and NMDARs (17, 35). We have shown that α2δ-1Tat peptide has no effect on VGCC currents and the Cavα1–α2δ-1 interaction (17, 35). In mouse brain slices, pretreatment with α2δ-1Tat peptide (1 μM for 30–60 min) abolished the TBS-induced increase in the amplitude of EPSPs in all MSNs (Fig. 3*A*). However, treatment with a Tat-fused scrambled control peptide (FGLGWQPWSLSFYLVWSGLILSVLHLIRSN) had no effect on the TBS-induced LTP of MSNs (Fig. 3*A*).

In addition, we used *Cacna2d1*-knockout mice (17, 33) to validate the critical role of α2δ-1 in TBS-induced LTP. TBS reliably induced LTP in all MSNs recorded in brain slices obtained from WT mice. In contrast, TBS did not significantly change the amplitude of EPSPs in any of the MSNs examined in *Cacna2d1*-knockout mice (Fig. 3*B*). Taken together, these findings indicate that α2δ-1 plays a pivotal role in TBS-induced corticostriatal LTP.

α2δ-1 is essential for increased presynaptic and postsynaptic NMDAR activity of MSNs by TBS

Because both α2δ-1 and NMDARs are required for TBS-induced LTP in the dorsomedial stratum, we determined to

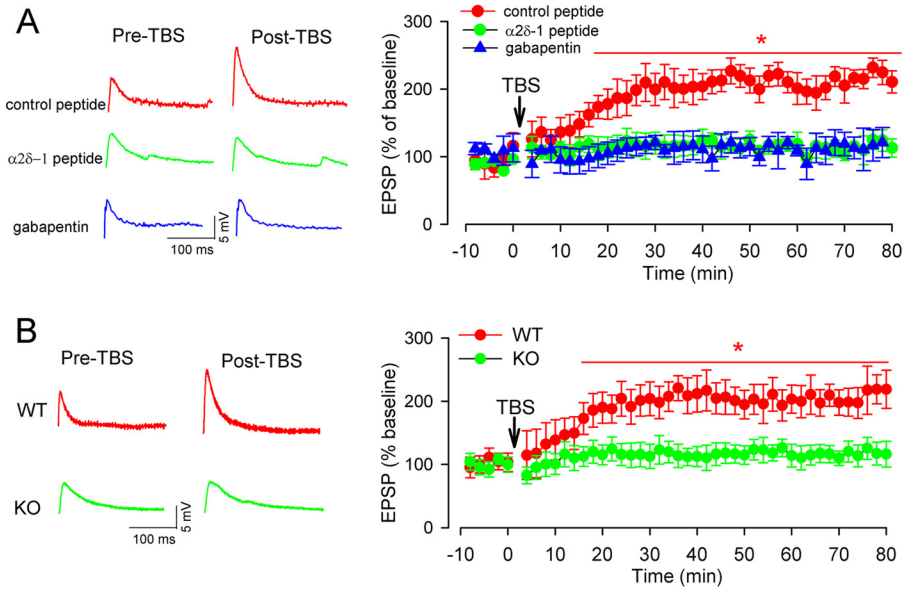

Figure 3. α2δ-1 is required for TBS-induced corticostriatal LTP of MSNs in the dorsomedial striatum. *A*, representative traces (20 min after TBS) and the time course of changes in EPSPs show the effect of treatment with gabapentin (100 μM for 30–60 min) or α2δ-1Tat peptide (1 μM for 30–60 min) on TBS-induced corticostriatal LTP of MSNs from WT mice ($n = 15$ neurons in each group). *B*, original recording traces (20 min post TBS) and the time course of changes in EPSPs show TBS-induced corticostriatal LTP in WT and *Cacna2d1*-knockout (KO) mice ($n = 15$ neurons in each group). The data are means ± S.E. *, $p < 0.05$ (*versus* baseline before TBS). One-way repeated measures of ANOVA followed by Dunnett's post hoc test was used.

what extent α2δ-1 is involved in the increased synaptic NMDAR activity of MSNs during LTP induction. To assess the presynaptic NMDAR activity of MSNs associated with TBS-induced LTP, we recorded miniature excitatory postsynaptic currents (mEPSCs), which reflect quantal glutamate release from presynaptic terminals (29, 36). The mEPSCs of MSNs were recorded at 20–30 min (at which time LTP was stably induced by TBS; Figs. 1 and 3) after TBS. In brain slices obtained from WT control mice, the frequency of mEPSCs of MSNs was low in the absence of TBS and was not significantly altered by bath application of 50 μM AP5 (Fig. 4, *A–C*). In contrast, TBS caused a large increase in the frequency, but not the amplitude, of mEPSCs in all MSNs of WT mice. In addition, this TBS-induced increase in mEPSC frequency was completely restored to the level of MSNs without TBS within 5 min after bath application of AP5 (Fig. 4, *A–C*). The baseline frequency and amplitude of mEPSCs in MSNs were comparable in WT and *Cacna2d1*-knockout mice. In brain slices from *Cacna2d1*-knockout mice, however, TBS failed to alter the frequency or amplitude of MSNs. Furthermore, bath application of AP5 had no effect on the frequency and amplitude of MSNs in brain slices from *Cacna2d1*-knockout mice, with or without TBS (Fig. 4, *A–C*).

To determine whether α2δ-1 is involved in the postsynaptic NMDAR activity augmented by TBS, we measured the current elicited by puff application of NMDA (37) directly onto the MSN being recorded. In MSNs from WT mice, puff application of 100 μM NMDA caused a much larger current amplitude 20–30 min after TBS than that without TBS (Fig. 4*D*). The baseline amplitude of currents elicited by the puff application of NMDA was similar in WT and *Cacna2d1*-knockout mice. However, in MSNs from *Cacna2d1*-knockout mice, TBS had no significant effect on the amplitude of currents elicited by puff application of NMDA compared with that without TBS (Fig. 4*D*). These data indicate that α2δ-1 is critically involved in the potentiated coincident presynaptic and postsynaptic NMDAR activity of MSNs during TBS-induced corticostriatal LTP.

α2δ-1 contributes to spatial learning and working memory

Adult WT and *Cacna2d1*-knockout mice were indistinguishable from one another on the basis of a visual inspection for overt abnormalities. We performed an open-field test to assess the exploration and locomotor activity of WT and *Cacna2d1*-knockout mice. WT and *Cacna2d1*-knockout mice did not show any significant difference in the total travel distance or the total time spent in the inner zone and outer zone (Fig. 5).

The electrophysiological studies described above demonstrate that TBS-induced corticostriatal LTP depends on α2δ-1–bound NMDARs. The NMDARs in the dorsomedial striatum play a crucial role in spatial learning and working memory (11, 38, 39). However, it is unclear whether α2δ-1–bound NMDARs are involved in this process. The natural tendency of rodents in a T-maze is to alternate their choice of goal arms, and spatial learning and working memory can be assessed using an alternation T-maze test (13, 38, 40). In our study, the mice were tested with a rewarded alternation T-maze task (five trials per day, 20-min intervals between trials) for five consecutive days. The percentage of correct alternations was recorded for each trial daily. Gabapentin (100 μg/kg, intraperitoneally) or vehicle (normal saline) was injected 20 min before the first trial each day. The mice injected with saline showed a gradual increase in the percentage of correct alternations in the second run of the T-maze task over 5 days (Fig. 6*A*). Compared with saline-treated mice, treatment with gabapentin significantly reduced the percentage of correct alternation in the T-maze task starting from day 3 (Fig. 6*A*).

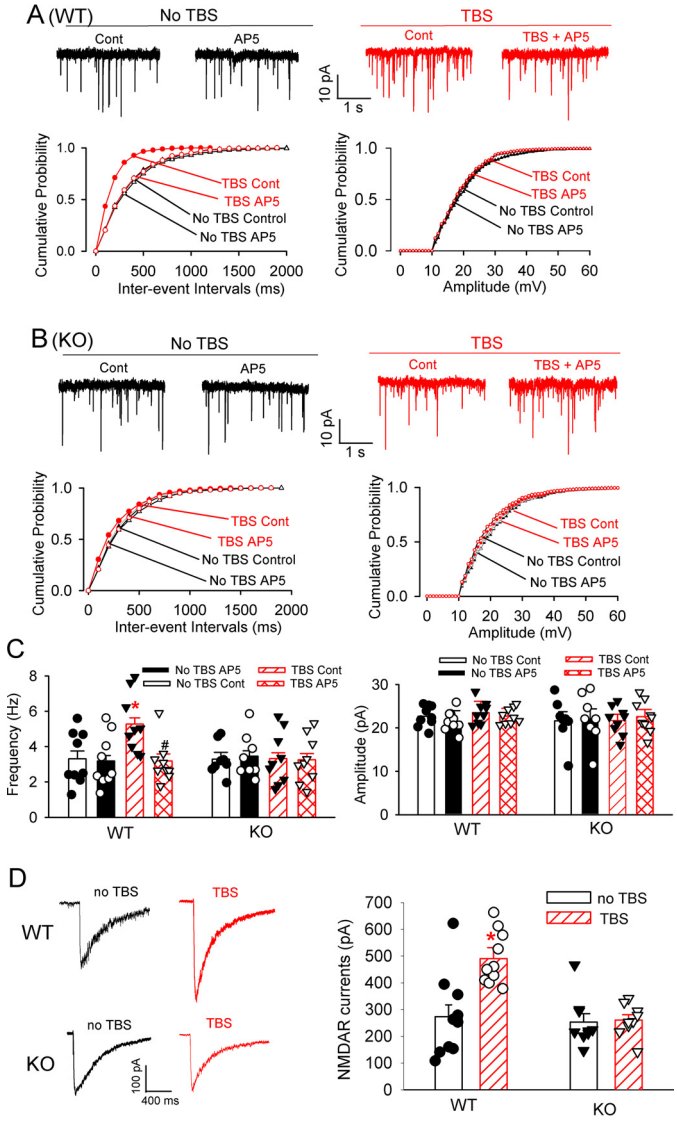

Figure 4. TBS increases the activity of presynaptic and postsynaptic NMDARs of MSNs in the dorsomedial striatum. *A* and *B*, representative traces and cumulative plots of mEPSCs during baseline control (*Cont*) and bath application of 50 μM AP5 show the effect of TBS or no TBS on mEPSCs of MSNs from WT and *Cacna2d1*-knockout (*KO*) mice. *C*, mean changes in the frequency and amplitude of mEPSCs in MSNs subjected to TBS or no TBS from WT and *Cacna2d1*-KO mice ($n = 10$ neurons in each group). *D*, representative recording traces and mean changes of puff NMDA-elicited NMDAR currents in MSNs subjected to TBS or no TB from WT and *Cacna2d1*-KO mice ($n = 10$ neurons in each group). The data are means ± S.E. *, $p < 0.05$ (*versus* baseline control in the no TBS group). #, $p < 0.05$ (*versus* baseline control in the TBS group). One-way ANOVA analysis followed by Tukey's post hoc test was used.

We also determined directly whether the α2δ-1–NMDAR complex in the dorsomedial striatum is involved in corticostriatal learning. The α2δ-1Tat peptide or control peptide (200 pmol, 200 nl) was microinjected bilaterally into the dorsomedial striatum through the implanted cannula 20 min before initiating each T-maze task training. Mice injected with the control peptide exhibited a steady increase in the percentage of correct alternations over 5 days of training. However, mice injected with α2δ-1Tat peptide showed a significant reduction in the percentage of correct alternation starting from day 3, compared with mice receiving the control peptide microinjection (Fig. 6*B*).

We next determined the potential difference between WT and *Cacna2d1*-knockout mice in the performance of the T-maze test. Both groups of mice were subjected to the alternation T-maze test for 5 consecutive days. The WT mice showed a gradual improvement in the correct turning response on the second run over 5 days (Fig. 6*C*). By comparison, the correct alternation of the T-maze task was significantly lower in *Cacna2d1*-knockout mice than in WT mice throughout the 5 days (Fig. 6*C*). These data collectively suggest that the α2δ-1–NMDAR complex in the dorsomedial striatum is critically involved in learning and memory.

α2δ-1 is involved in motor skill learning

The NMDARs in the dorsal striatum also contribute to motor skill learning (11, 41). Thus, we used the accelerating rotarod test (three trials per day, with a 20-min interval between trials, for 2 consecutive days) to determine the role of α2δ-1 in motor coordination learning. Gabapentin (100 μg/kg, intraperitoneally) or vehicle saline was injected 20 min before the first trial each day. Mice receiving saline injection showed a gradual increase in the latency to fall from the rotarod over the six trials (Fig. 7*A*). Although the two groups of mice exhibited increased durations on the rotating cylinder with successive trials, the falling latency was significantly shorter in mice receiving gabapentin treatment than in those injected with vehicle at trials 3–6 (Fig. 7*A*).

We then determined whether the α2δ-1–NMDAR complex in the dorsomedial striatum is involved in the motor learning. The control peptide or α2δ-1Tat peptide (200 pmol, 200 nl) was microinjected bilaterally into the dorsomedial striatum 20 min before each training. Mice injected with the control peptide displayed a continuing increase in the falling latency with successive trials (Fig. 7*B*). By comparison, mice injected with α2δ-1Tat peptide showed a significantly lower improvement in the falling latency (Fig. 7*B*).

In addition, we used the accelerating rotarod test to evaluate motor learning in WT and *Cacna2d1*-knockout mice. Both groups of mice showed an incremental increase in the latency to fall from the rotarod over the six successive trials (Fig. 7*C*). However, *Cacna2d1*-knockout mice had significantly less time on the rotarod than did WT mice throughout the six trials (Fig. 7*C*). Together, these results strongly suggest that α2δ-1–bound NMDARs in the striatum contribute to working memory and motor learning.

Discussion

The striatum is well-known for its role in developing habits and acquiring motor skills (42, 43). Striatum learning requires changes in the strength of synaptic connections during the memorization of a complex task. The LTP of excitatory cortical afferents to the dorsal striatum likely occurs when learning to encode new skills and habits (44, 45). Activation of cortical afferents with the theta-ranged frequency can induce corticostriatal LTP in striatal MSNs *in vivo* (45) and in brain slices in the physiological Mg^{2+} concentration (7, 8). Blocking or genetically deleting NMDARs can prevent corticostriatal LTP induced by TBS (7, 8). The theta-burst rhythm is considered a naturally occurring cell activity pattern, and TBS exploits the

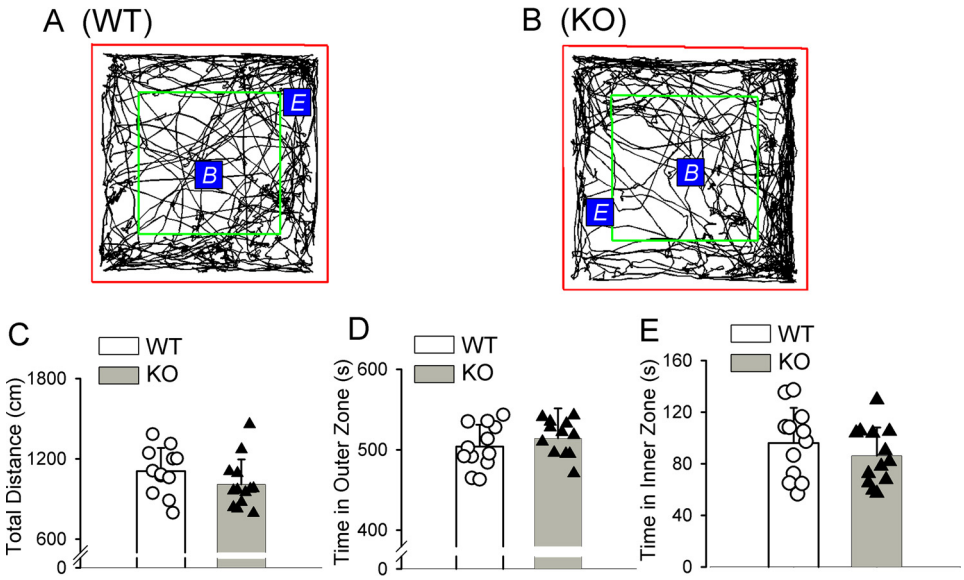

Figure 5. The exploration and locomotor activity of WT and *Cacna2d1*-knockout mice subjected to the open-field test. *A* and *B*, representative tracks of WT and *Cacna2d1*-knockout (*KO*) mice subjected to open field test for 10 min. The *red square* was the open-field testing area. Within the entire testing area, the area *inside* the *green square* was defined as the inner zone, and the space *outside* of the *green square* was the outer zone. The beginning point *B* and the ending point *E* are indicated in the representative tracks. *C–E*, bar graphs and scatter plots show the total travel distances and the time spent in the outer and inner zones in WT and KO mice subjected to the 10-min open field test ($n = 12$ mice in the WT group; $n = 13$ mice in the KO group). The data are means ± S.E.

endogenous circuit properties to maximize NMDAR activation with the least amount of afferent stimulation (46). In corticostriatal LTP induction, the enhanced presynaptic NMDAR activity augments glutamate release from cortical afferent terminals through Ca^{2+} influx (7). We demonstrated that blocking postsynaptic NMDARs also completely blocked corticostriatal LTP in MSNs. Furthermore, we showed that TBS caused a large increase in the activity of presynaptic and postsynaptic NMDARs in corticostriatal synapses. These findings strongly suggest that TBS-induced corticostriatal LTP is associated with the potentiated activity of both presynaptic and postsynaptic NMDARs.

α2δ-1 is expressed in distinct brain regions involved in learning and memory, including the cortex, hippocampus, and striatum (21, 22). α2δ-1 may interact with thrombospondin, an astrocyte-secreted protein, to affect synaptogenesis (but not already-formed synapses) (47). However, the results of a recent study suggest that the association between α2δ-1 and thrombospondin is rather weak and that there is no α2δ-1-thrombospondin interaction on the cell surface (48). α2δ-1 also interacts with BK channels to indirectly modulate VGCC activity (49), although this interaction may not be relevant to TBS-induced LTP. In this study, we showed that α2δ-1 physically interacted with NMDARs in the striatum in both mice and humans. This finding is consistent with the results of our recent studies showing that α2δ-1 interacts directly with NMDARs to promote their synaptic trafficking in the spinal cord and brain (17, 35, 50, 51). We showed that α2δ-1 protein was not detected in flow-through membrane protein samples after further immunoprecipitation with the GluN1 antibody. These data suggest that most, if not all, α2δ-1 membrane proteins in the striatum may be associated with NMDARs. Importantly, we found that targeting α2δ-1–bound NMDARs with gabapentin or α2δ-1Tat peptide abolished TBS-induced corticostriatal LTP. In addition, TBS was unable to induce LTP in the corticostriatal synapses of *Cacna2d1*-knockout mice. Therefore, the switch from α2δ-1–free to α2δ-1–bound NMDARs plays an obligatory role in corticostriatal LTP induced by TBS.

The most striking finding of our study is that TBS-induced corticostriatal LTP depends on α2δ-1–bound NMDARs at both presynaptic and postsynaptic sites. Activation of NMDARs is a critical requirement for the induction of LTP at corticostriatal synapses (7, 8). Although postsynaptic NMDARs of MSNs are tonically active, blocking NMDARs had no effect on the baseline frequency of mEPSCs in MSNs in the absence of TBS, suggesting that presynaptic NMDARs are normally latent and not functionally active under basal conditions. We demonstrated that TBS increased the activity of both presynaptic and postsynaptic NMDARs in corticostriatal synapses. Thus, TBS-induced corticostriatal LTP may depend on coincident activity in presynaptic and postsynaptic neurons, resulting in calcium influx through synaptic NMDARs. Sustained synaptic glutamate release via presynaptic NMDAR activation can lead to long-lasting stimulation of postsynaptic NMDARs, which can activate calcium-dependent signaling, including AMPA receptor insertion and lasting structural changes at dendritic spines (52–54). We showed that inhibiting α2δ-1 activity with gabapentin, interfering with the α2δ-1–NMDAR interaction using α2δ-1Tat peptide, and genetic ablation of α2δ-1 completely blocked the increase in presynaptic and postsynaptic NMDAR activity during LTP induction. These findings clearly indicate that α2δ-1–bound NMDARs account for most, if not all, increased NMDAR activity by TBS at the corticostriatal synapses. Therefore, α2δ-1–bound NMDARs are required for the coordination of functional changes in synaptic efficacy in TBS-induced LTP.

Another major finding of our study is that targeting the α2δ-1–NMDAR complex in the dorsomedial striatum or the aboli-

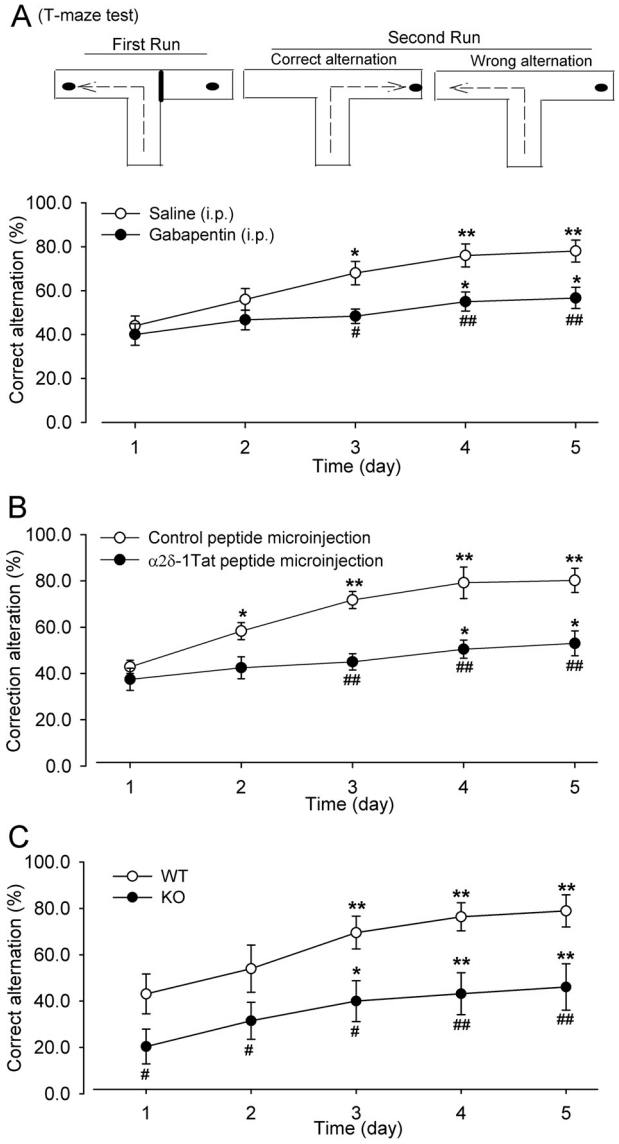

Figure 6. α2δ-1 contributes to spatial learning and memory. *A*, mean changes show the effect of gabapentin (100 mg/kg, intraperitoneally) on the correct alternation of mice subjected to the T-maze test over 5 consecutive days ($n = 10$ mice in each group). A schematic diagram of the T-maze test is shown at the *top*. *B*, mean changes show the effect of α2δ-1Tat peptide (200 pmol, 200 nl) microinjected into the dorsomedial striatum on the correct alternation of mice subjected to the T-maze test over 5 consecutive days ($n = 7$ mice in the control peptide group; $n = 8$ mice in the α2δ-1Tat peptide group). *C*, mean changes of correct alternation in WT and *Cacna2d1*-knockout (*KO*) mice subjected to the T-maze test over 5 consecutive days ($n = 13$ mice in each group). The data are means ± S.E. *, $p < 0.05$; **$p < 0.01$ (*versus* respective values on day 1); #, $p < 0.05$; ##, $p < 0.01$ (*versus* respective values on the same day in the saline, control peptide, or WT group). Two-way ANOVA analysis followed by Tukey's post hoc test was used.

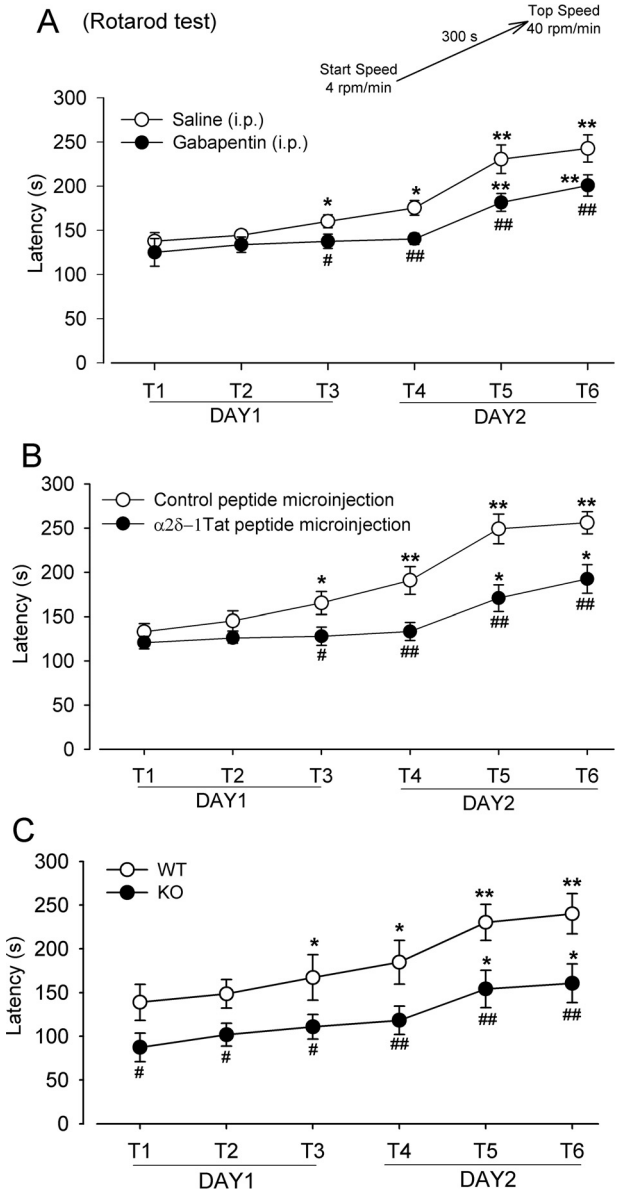

Figure 7. α2δ-1 is involved in motor learning. *A*, mean changes show the effect of gabapentin (100 mg/kg, intraperitoneally) on the falling latency of mice during six rotarod test trials (T1–T6) over 2 consecutive days ($n = 10$ mice in each group). The rotarod test protocol is depicted at the *top*. *B*, mean changes show the effect of α2δ-1Tat peptide (200 pmol, 200 nl) microinjected into the dorsomedial striatum on the falling latency of mice during six rotarod test trials (T1–T6) over two consecutive days ($n = 7$ mice in the control peptide group; $n = 8$ mice in the α2δ-1Tat peptide group). *C*, mean changes in the falling latency in WT and *Cacna2d1*-knockout (*KO*) mice subjected to six rotarod test trials (T1–T6) over 2 consecutive days ($n = 10$ mice in each group). The data are means ± S.E. *, $p < 0.05$; **, $p < 0.01$ (*versus* respective values at T1). #, $p < 0.05$; ##, $p < 0.01$ (*versus* respective values in the same trial in the saline, control peptide, or WT group). Two-way ANOVA analysis followed by Tukey's post hoc test was used.

tion of α2δ-1 attenuates performance on T-maze and rotarod tests, both of which are associated with striatum-based learning and memory. These findings support the notion that α2δ-1–bound NMDARs contribute to learning and memory. The dorsomedial striatum lesions impair the acquisition of spatial alternation behavior by disrupting the signal necessary to link a goal with a specific spatial sequence (13, 38, 55). The NMDARs in the dorsal striatum are involved in learning and memory (11, 39, 56). It should be noted that learning and memory involve neural circuits among the cortex, hippocampus, and striatum that coordinate information storage, retrieval, and manipulation to correlate task performance (1, 55, 57). Because α2δ-1 is extensively expressed in the cortex, amygdala, and hippocampus, α2δ-1–bound NMDARs in these brain regions are also likely involved in various learning, association, motivational, and cognitive functions.

In summary, we provide new evidence that α2δ-1 is essential for corticostriatal LTP induction through its interaction with

NMDARs. α2δ-1 may mobilize and recruit NMDARs at both presynaptic and postsynaptic sites during TBS-induced corticostriatal LTP. Our findings reveal a critical role for α2δ-1 in dynamic NMDAR regulation in LTP induction and in learning and memory. This information provides new insight into the molecular mechanism that is fundamentally important for synaptic plasticity and the associated learning and memory.

Experimental procedures

Animals

All surgical procedures and protocols were approved by the Animal Care and Use Committee of the University of Texas M. D. Anderson Cancer Center. Adult male and female mice (8–10 weeks old), housed three to four per cage, were used for final experiments. WT and *Cacna2d1*-knockout mice (C57BL/6 genetic background) were generated as described previously (33). Two breeding pairs of heterozygous (*Cacna2d1*$^{+/-}$) mice were purchased from Medical Research Council (Harwell Didcot, Oxfordshire, UK), and *Cacna2d1*$^{-/-}$ mice (knockout) and *Cacna2d1*$^{+/+}$ (WT) littermates were obtained by breeding the heterozygous mice. The animals were ear-marked at the time of weaning (21–23 days after birth), and tail biopsies were used for genotyping. The housing room was maintained at 23 °C on a 12-h light/dark cycle.

Co-immunoprecipitation of GluN1 and α2δ-1 in the striatum tissue

We obtained frozen human striatum tissues (two males and two females; age range, 66–77 years) from the Harvard Brain Tissue Resources Center, a NeuroBioBank Repository funded by the National Institutes of Health. The striatum tissues from humans and mice were dissected and homogenized in ice-cold hypotonic buffer (20 mM Tris, 1 mM $CaCl_2$, 1 mM $MgCl_2$, and protease inhibitors, pH 7.4). The nuclei and large debris were removed by centrifugation at 300 × *g* for 5 min. The supernatant was centrifuged for 20 min at 21,000 × *g*. The pellets were resuspended and solubilized in immunoprecipitation buffer (50 mM Tris, 250 mM NaCl, 10% glycerol, 0.5% Nonidet P-40, 20 mM NaF, 1 mM Na_3VO_4, 10 mM *N*-ethylmaleimide, 1 mM phenylmethylsulfonyl fluoride, 2 mM benzamide, and protease inhibitors, pH 7.4). The membrane protein was incubated at 4 °C overnight with protein A/G beads (catalog no. 16-266, Millipore) prebound to the mouse anti–α2δ-1 (catalog no. sc-271697, Santa Cruz Biotechnology, Dallas, TX). Protein A/G beads prebound to mouse IgG were used as controls. The samples were washed five times with immunoprecipitation buffer and then immunoblotted. Furthermore, flow-through samples containing the same amount of proteins were incubated at 4 °C overnight with protein A/G beads prebound to the mouse anti-GluN1 antibody (catalog no. 75-272, NeuroMab, Davis, CA). GluN1 and α2δ-1 protein bands were detected using Western immunoblotting. The following antibodies were selected for immunoblotting and validated in our previous study (17): rabbit anti–α2δ-1 (catalog no. C5105, 1:1,000, Sigma–Aldrich) and rabbit anti-GluN1 (catalog no. G8913, 1:1,000, Sigma–Aldrich). The protein bands were visualized with an ECL kit (Thermo Fisher Scientific), and protein-band intensity was visualized and quantified using the Odyssey Fc Imager (LI-COR Biosciences, Lincoln, NE).

Brain slice preparation

Under deep anesthesia with 5% isoflurane, the mice were decapitated; their brains were quickly removed and placed into ice-cold artificial cerebrospinal fluid composed of 124.0 mM NaCl, 3.0 mM KCl, 1.3 mM $MgSO_4$, 2.4 mM $CaCl_2$, 1.4 mM NaH_2PO_4, 10.0 mM glucose, and 26.0 mM $NaHCO_3$, which was saturated with a mixture of 95% O_2 and 5% CO_2. The tissue block was fixed on the stage of vibratome (Leica) and sagittally sectioned into 300-μm-thick slices. The striatum slices were then transferred into 32 °C artificial cerebral spinal fluid that was continuously oxygenated with a mixture of 95% O_2 and 5% CO_2 and incubated for at least 1 h before the electrophysiological recording was obtained. The slices were placed in the recording chamber, fixed, and perfused at 3 ml/min with oxygenated artificial cerebral spinal fluid at a temperature of 34 °C, maintained using an inline solution heater. The recording electrodes were pulled from borosilicate glasses with a final resistance of 3–5 MΩ when filled with the following intracellular solution: 140.0 mM potassium gluconate, 2.0 mM $MgCl_2$, 0.1 mM $CaCl_2$, 10.0 mM HEPES, 1.1 mM EGTA, 0.3 mM Na_2-GTP, and 2.0 mM Na_2-ATP adjusted to pH 7.25 with 1 M KOH, 270–290 mOsm. The whole-cell recordings were performed using a Multiclamp 700B amplifier (Molecular Devices), and all signals were filtered at 2 kHz, digitized at 20 kHz using Digidata 1320A, and stored on the computer for off-line analysis. The medium spiny neurons (MSNs) in the dorsomedial striatum were visualized by IR differential interference optics with a water-immersion objective. MSNs were also identified by their intrinsic membrane properties: resting membrane potential more negative than −80 mV, inward and outward rectification in response to somatic current injection, and a long depolarization ramp to the action potential threshold leading to a delayed spike discharge (27, 28).

LTP induction

Electrical stimulation was applied to elicit LTP using a tungsten bipolar electrode placed on cortical layer VI close to the white matter (8). After a whole-cell recording was made from MSNs in the dorsomedial striatum, a "test" stimulus was applied at 0.017 Hz to elicit EPSPs. The duration of all stimulation pulses was 0.1 ms, and the stimulation intensity was adjusted to a level at which the baseline EPSP amplitude was ~5 mV. Recordings were rejected if the peak amplitude of baseline EPSPs was less than 2 mV, if the resting membrane potential changed by more than 10%, or if the input resistance changed more than 30% during recordings. The stable responses were recorded for at least 10 min before applying TBS, which consisted of 10 trains of stimuli (each train contained bursts of 4 spikes at 100 Hz, and the bursts repeated 10 times at 5 Hz) at 10-s intervals (8). The intensity and pulse duration of stimulation for baseline and LTP induction were kept the same for the same neurons. After TBS, EPSP were continuously recorded for at least another 80 min with a single stimulus pulse at 0.017 Hz, and the EPSP amplitude was analyzed using MiniAnalysis software (Synaptosoft, Inc., Decatur, GA). All experiments

were performed in artificial cerebrospinal fluid containing normal Mg^{2+} and in the presence of picrotoxin (100 μM) to eliminate GABAergic input (7, 8). Gabapentin was purchased from Tocris Bioscience (Bristol, UK), and α2δ-1Tat peptide and control peptide were synthesized by Bio Basic Inc. (Marham, Ontario, Canada) and validated using LC and MS.

Recording presynaptic and postsynaptic NMDAR activity

The mEPSCs were recorded from MSNs in the dorsomedial striatum at a holding potential −60 mV in the presence of 1 μM tetrodotoxin (37, 58). The intracellular solutions contained 140.0 mM potassium gluconate, 2.0 mM $MgCl_2$, 0.1 mM $CaCl_2$, 10.0 mM HEPES, 1.1 mM EGTA, 0.3 mM Na_2-GTP, and 2.0 mM Na_2-ATP adjusted to pH 7.25 with 1 M KOH, 270–290 mOsm. The mEPSCs were analyzed, and cumulative responses of frequency and amplitude were calculated using MiniAnalysis software (Synaptosoft, Inc.). To measure postsynaptic NMDAR activity, puff NMDA-elicited currents were recorded in MSNs. In brief, NMDAR currents were recorded at a holding potential of −60 mV and elicited by puff application of NMDA through a Pressure System IIe (Toohey Company, Fairfield, NJ). The puff pipette (15-μm tip diameter) was placed ~150 μm away from the recorded cells. Positive pressure (3 p.s.i.) was applied (durations of 200 ms) to eject NMDA (100 μM) onto the recorded cell to elicit currents with the intracellular solution containing QX314, a sodium channel blocker. Because the NMDAR channel is voltage-dependently blocked by Mg^{2+} at a negative holding potential and co-activated by glycine, puff NMDA-elicited currents were recorded in Mg^{2+}-free solution and in the presence of 10 μM glycine (37). In all electrophysiological experiments, only one neuron was recorded from each hemislice, and at least three mice were included for recording in each group.

Cannula implantation and microinjection

The mice were anesthetized via inhaling 1–2% isoflurane, and their heads were stereotaxically fixed using the adapter and ear bars. An incision was made along the middle line on the head, and two small holes were drilled at the coordinates: anteroposterior +0.5 mm and mediolateral 1.5 mm. The guide cannulas were bilaterally implanted dorsally and fixed using the dental acrylic cement. The guide cannula was made of stainless steel (2.3 mm long, catalog no. 62004, RWD Life Science Inc., San Diego, CA). A dummy cannula was kept in the guide cannula for 10 days before conducting behavioral tests. For the dorsomedial microinjection, the mice were briefly anesthetized with 1% isoflurane. The injection cannula (diameter, 0.11 mm) was 0.5 mm longer than the guide cannula. The dorsomedial striatum was targeted at anteroposterior +0.5 mm, mediolateral 1.5 mm, and dorsoventral −2.8 mm (59). Each microinjection took ~3 min. At the end of the behavioral tests, red FluoSpheres (0.4 μm, 100 nl) were bilaterally microinjected into the dorsomedial striatum in each mouse. The brain was fixed with 4% paraformaldehyde for 72 h and coronally cut to 50-μm-thick slices to confirm the injection site. We excluded the respective behavioral data if the microinjection missed the dorsomedial striatum in mice.

Open-field test

The open-field test was performed in a quiet behavioral testing room to examine the exploration and locomotor activity of mice (60). The mice were allowed to acclimate in the room for 30 min before starting the test. The size of the plastic open-field box is 40 cm × 40 cm × 35 cm (Noldus, Boston, MA). The central inner zone was defined as a square of 24 cm × 24 cm within the open-field testing area, whereas the remaining outer space was marked as the outer zone. The open-field testing area was wiped with 95% ethanol before each test. The mice were placed in the middle of the testing area and allowed to move freely for 10 min. The travel path of each mice was video-recorded using a GigE color camera (Noldus). The total travel distance and total time spent in the inner zone and outer zone for each mice were analyzed using Autotyping software (61).

Rewarded alternation T-maze test

The mice were initially food-restricted for 5 days to achieve 85–90% of their free body weight (40). The mice were trained to habituate in a T-maze apparatus with two open-side (goal) arms for 3 min, twice a day with a 30-min interval, for 5 days before starting the appetite-motivated T-maze task. The test contained five trials at 20-min intervals for 5 consecutive days. Each trial was composed of two runs in order. On the first run, the correct arm (closed) was randomly defined to avoid adaption. The mouse was placed in the start area at the bottom of T-maze stem, and the door in the start area was opened to allow the mouse to explore the chocolate reward at the end of the opened arm. After the reward had been completely consumed, the mice were guided back to the start area for the second run. On the second run, the correct arm was also opened, and the mouse had to choose between the previously entered arm and the correct arm. If it entered the correct arm (correct alternation), it was given time to completely consume the chocolate reward; if not, the mouse received no reward. No more than 2 min was spent in each trial. For five trials conducted each day, the percentage of correct alternation was calculated for each mouse (40). During the T-maze test, the mice were weighed every day to verify maintenance of 85–90% of their free body weight.

Rotarod performance test

The rotarod test was conducted in mice using an accelerating rotarod (IITC Life Science, Woodland Hills, CA). The mice were initially placed on a rotarod opposite to the rotating direction. The initial rotating speed was 4 rpm/min, which progressively increased to a maximum of 40 rpm/min over 300 s for each trial (41, 62). Each animal was given three trials at 20-min intervals per day for 2 consecutive days. Overall performance was expressed as the latency to fall from the accelerating rotating rod. These latencies were automatically detected and measured using a timer built into the apparatus. The mouse was given a new trial if it immediately fell down at the beginning of each trial.

Study design and statistical analysis

All data were presented as means ± S.E. No statistical methods were used to predetermine sample sizes for biochemical

studies, but our sample sizes were similar to those generally employed in the field. For proper exclusion of data points, the criteria were established before data collection. In electrophysiological recording experiments, we monitored cell capacitance, input resistance, series resistance, resting membrane potential, and baseline holding current. We excluded cells if the recording indicated a rundown condition. The peak amplitude of EPSPs and puff NMDAR currents was determined and analyzed using pClamp 10 (Molecular Devices). The amplitude and frequency of mEPSCs were analyzed with a peak detection program (MiniAnalysis, Synaptosoft, Leonia, NJ). Detection of events was accomplished by setting a threshold above the noise level. The distribution cumulative probability of the amplitude and interevent interval of mEPSCs was compared using the Komogorov–Smirnov test, which estimates the probability that two cumulative distributions are similar. The behavioral test and electrophysiological data were analyzed using one-way ANOVA followed by Dunnett's and Tukey's post hoc tests or two-way ANOVA followed by Tukey's post hoc test. $p < 0.05$ was considered statistically significant.

Author contributions—J.-J. Z., D.-P. L., S.-R. C., and Y. L. data curation; J.-J. Z., D.-P. L., and S.-R. C. investigation; J.-J. Z. and H.-L. P. writing-original draft; H.-L. P. conceptualization; H.-L. P. supervision; H.-L. P. project administration; H.-L. P. writing-review and editing.

Acknowledgments—Human brain tissues were obtained from the Harvard Brain Tissue Resources Center, a NeuroBioBank Repository funded by the National Institutes of Health.

References

1. Pennartz, C. M., Berke, J. D., Graybiel, A. M., Ito, R., Lansink, C. S., van der Meer, M., Redish, A. D., Smith, K. S., and Voorn, P. (2009) Corticostriatal interactions during learning, memory processing, and decision making. *J. Neurosci.* **29,** 12831–12838 CrossRef Medline
2. Yin, H. H., and Knowlton, B. J. (2006) The role of the basal ganglia in habit formation. *Nat. Rev. Neurosci.* **7,** 464–476 CrossRef Medline
3. Yin, H. H., Ostlund, S. B., and Balleine, B. W. (2008) Reward-guided learning beyond dopamine in the nucleus accumbens: the integrative functions of cortico-basal ganglia networks. *Eur. J. Neurosci.* **28,** 1437–1448 CrossRef Medline
4. Charpier, S., and Deniau, J. M. (1997) *In vivo* activity-dependent plasticity at cortico-striatal connections: evidence for physiological long-term potentiation. *Proc. Natl. Acad. Sci. U.S.A.* **94,** 7036–7040 CrossRef Medline
5. Mahon, S., Deniau, J. M., and Charpier, S. (2004) Corticostriatal plasticity: life after the depression. *Trends Neurosci.* **27,** 460–467 CrossRef Medline
6. Partridge, J. G., Tang, K. C., and Lovinger, D. M. (2000) Regional and postnatal heterogeneity of activity-dependent long-term changes in synaptic efficacy in the dorsal striatum. *J. Neurophysiol.* **84,** 1422–1429 CrossRef Medline
7. Park, H., Popescu, A., and Poo, M. M. (2014) Essential role of presynaptic NMDA receptors in activity-dependent BDNF secretion and corticostriatal LTP. *Neuron* **84,** 1009–1022 CrossRef Medline
8. Hawes, S. L., Gillani, F., Evans, R. C., Benkert, E. A., and Blackwell, K. T. (2013) Sensitivity to theta-burst timing permits LTP in dorsal striatal adult brain slice. *J. Neurophysiol.* **110,** 2027–2036 CrossRef Medline
9. Calabresi, P., Pisani, A., Mercuri, N. B., and Bernardi, G. (1996) The corticostriatal projection: from synaptic plasticity to dysfunctions of the basal ganglia. *Trends Neurosci.* **19,** 19–24 CrossRef Medline
10. Graybiel, A. M. (1990) Neurotransmitters and neuromodulators in the basal ganglia. *Trends Neurosci.* **13,** 244–254 CrossRef Medline
11. Dang, M. T., Yokoi, F., Yin, H. H., Lovinger, D. M., Wang, Y., and Li, Y. (2006) Disrupted motor learning and long-term synaptic plasticity in mice lacking NMDAR1 in the striatum. *Proc. Natl. Acad. Sci. U.S.A.* **103,** 15254–15259 CrossRef Medline
12. Hauber, W., and Schmidt, W. J. (1989) Effects of intrastriatal blockade of glutamatergic transmission on the acquisition of T-maze and radial maze tasks. *J. Neural. Transm. Gen. Sect.* **78,** 29–41 CrossRef Medline
13. Yin, H. H., and Knowlton, B. J. (2004) Contributions of striatal subregions to place and response learning. *Learn. Mem.* **11,** 459–463 CrossRef Medline
14. Dolphin, A. C. (2012) Calcium channel auxiliary α2δ and beta subunits: trafficking and one step beyond. *Nat. Rev. Neurosci.* **13,** 542–555 CrossRef Medline
15. Müller, C. S., Haupt, A., Bildl, W., Schindler, J., Knaus, H. G., Meissner, M., Rammner, B., Striessnig, J., Flockerzi, V., Fakler, B., and Schulte, U. (2010) Quantitative proteomics of the Cav2 channel nano-environments in the mammalian brain. *Proc. Natl. Acad. Sci. U.S.A.* **107,** 14950–14957 CrossRef Medline
16. Felsted, J. A., Chien, C. H., Wang, D., Panessiti, M., Ameroso, D., Greenberg, A., Feng, G., Kong, D., and Rios, M. (2017) α2δ-1 in $SF1^+$ neurons of the ventromedial hypothalamus is an essential regulator of glucose and lipid homeostasis. *Cell Reports* **21,** 2737–2747 CrossRef Medline
17. Chen, J., Li, L., Chen, S. R., Chen, H., Xie, J. D., Sirrieh, R. E., MacLean, D. M., Zhang, Y., Zhou, M. H., Jayaraman, V., and Pan, H. L. (2018) The α2δ 1–NMDA receptor complex is critically involved in neuropathic pain development and gabapentin therapeutic actions. *Cell Rep.* **22,** 2307–2321 CrossRef Medline
18. Hoppa, M. B., Lana, B., Margas, W., Dolphin, A. C., and Ryan, T. A. (2012) α2δ expression sets presynaptic calcium channel abundance and release probability. *Nature* **486,** 122–125 CrossRef Medline
19. Schumacher, T. B., Beck, H., Steinhäuser, C., Schramm, J., and Elger, C. E. (1998) Effects of phenytoin, carbamazepine, and gabapentin on calcium channels in hippocampal granule cells from patients with temporal lobe epilepsy. *Epilepsia* **39,** 355–363 CrossRef Medline
20. Cassidy, J. S., Ferron, L., Kadurin, I., Pratt, W. S., and Dolphin, A. C. (2014) Functional exofacially tagged N-type calcium channels elucidate the interaction with auxiliary α2δ-1 subunits. *Proc. Natl. Acad. Sci. U.S.A.* **111,** 8979–8984 CrossRef Medline
21. Cole, R. L., Lechner, S. M., Williams, M. E., Prodanovich, P., Bleicher, L., Varney, M. A., and Gu, G. (2005) Differential distribution of voltage-gated calcium channel alpha-2 delta (α2δ) subunit mRNA-containing cells in the rat central nervous system and the dorsal root ganglia. *J. Comp. Neurol.* **491,** 246–269 CrossRef Medline
22. Taylor, C. P., and Garrido, R. (2008) Immunostaining of rat brain, spinal cord, sensory neurons and skeletal muscle for calcium channel alpha2-delta (α2δ) type 1 protein. *Neuroscience* **155,** 510–521 CrossRef Medline
23. Chen, L., Chetkovich, D. M., Petralia, R. S., Sweeney, N. T., Kawasaki, Y., Wenthold, R. J., Bredt, D. S., and Nicoll, R. A. (2000) Stargazin regulates synaptic targeting of AMPA receptors by two distinct mechanisms. *Nature* **408,** 936–943 CrossRef Medline
24. DeCoteau, W. E., Thorn, C., Gibson, D. J., Courtemanche, R., Mitra, P., Kubota, Y., and Graybiel, A. M. (2007) Oscillations of local field potentials in the rat dorsal striatum during spontaneous and instructed behaviors. *J. Neurophysiol.* **97,** 3800–3805 CrossRef Medline
25. Tort, A. B., Kramer, M. A., Thorn, C., Gibson, D. J., Kubota, Y., Graybiel, A. M., and Kopell, N. J. (2008) Dynamic cross-frequency couplings of local field potential oscillations in rat striatum and hippocampus during performance of a T-maze task. *Proc. Natl. Acad. Sci. U.S.A.* **105,** 20517–20522 CrossRef Medline
26. Tepper, J. M., and Bolam, J. P. (2004) Functional diversity and specificity of neostriatal interneurons. *Curr. Opin. Neurobiol.* **14,** 685–692 CrossRef Medline
27. Jia, Y., Gall, C. M., and Lynch, G. (2010) Presynaptic BDNF promotes postsynaptic long-term potentiation in the dorsal striatum. *J. Neurosci.* **30,** 14440–14445 CrossRef Medline
28. Kawaguchi, Y., Wilson, C. J., and Emson, P. C. (1989) Intracellular recording of identified neostriatal patch and matrix spiny cells in a slice prepa-

ration preserving cortical inputs. *J. Neurophysiol.* **62,** 1052–1068 CrossRef Medline
29. Zhou, H. Y., Chen, S. R., Chen, H., and Pan, H. L. (2010) Opioid-induced long-term potentiation in the spinal cord is a presynaptic event. *J. Neurosci.* **30,** 4460–4466 CrossRef Medline
30. Allison, D. W., Gelfand, V. I., Spector, I., and Craig, A. M. (1998) Role of actin in anchoring postsynaptic receptors in cultured hippocampal neurons: differential attachment of NMDA versus AMPA receptors. *J. Neurosci.* **18,** 2423–2436 CrossRef Medline
31. Tovar, K. R., and Westbrook, G. L. (2002) Mobile NMDA receptors at hippocampal synapses. *Neuron* **34,** 255–264 CrossRef Medline
32. Li, D. P., Zhu, L. H., Pachuau, J., Lee, H. A., and Pan, H. L. (2014) mGluR5 Upregulation increases excitability of hypothalamic presympathetic neurons through NMDA receptor trafficking in spontaneously hypertensive rats. *J. Neurosci.* **34,** 4309–4317 CrossRef Medline
33. Fuller-Bicer, G. A., Varadi, G., Koch, S. E., Ishii, M., Bodi, I., Kadeer, N., Muth, J. N., Mikala, G., Petrashevskaya, N. N., Jordan, M. A., Zhang, S. P., Qin, N., Flores, C. M., Isaacsohn, I., Varadi, M., *et al.* (2009) Targeted disruption of the voltage-dependent calcium channel α2/δ-1-subunit. *Am. J. Physiol. Heart Circ. Physiol.* **297,** H117–H124 CrossRef Medline
34. Gee, N. S., Brown, J. P., Dissanayake, V. U., Offord, J., Thurlow, R., and Woodruff, G. N. (1996) The novel anticonvulsant drug, gabapentin (Neurontin), binds to the α2δ subunit of a calcium channel. *J. Biol. Chem.* **271,** 5768–5776 CrossRef Medline
35. Luo, Y., Ma, H., Zhou, J. J., Li, L., Chen, S. R., Zhang, J., Chen, L., and Pan, H. L. (2018) Focal cerebral ischemia and reperfusion induce brain injury through α2δ-1–bound NMDA receptors. *Stroke* **49,** 2464–2472 CrossRef Medline
36. Li, L., Chen, S. R., Chen, H., Wen, L., Hittelman, W. N., Xie, J. D., and Pan, H. L. (2016) Chloride homeostasis critically regulates synaptic NMDA receptor activity in neuropathic pain. *Cell Rep.* **15,** 1376–1383 CrossRef Medline
37. Li, D. P., Zhou, J. J., Zhang, J., and Pan, H. L. (2017) CaMKII regulates synaptic NMDA receptor activity of hypothalamic presympathetic neurons and sympathetic outflow in hypertension. *J. Neurosci.* **37,** 10690–10699 CrossRef Medline
38. Palencia, C. A., and Ragozzino, M. E. (2004) The influence of NMDA receptors in the dorsomedial striatum on response reversal learning. *Neurobiol. Learn. Mem.* **82,** 81–89 CrossRef Medline
39. Yin, H. H., Knowlton, B. J., and Balleine, B. W. (2005) Blockade of NMDA receptors in the dorsomedial striatum prevents action-outcome learning in instrumental conditioning. *Eur. J. Neurosci.* **22,** 505–512 CrossRef Medline
40. Deacon, R. M., and Rawlins, J. N. (2006) T-maze alternation in the rodent. *Nat. Protoc.* **1,** 7–12 CrossRef Medline
41. Lemay-Clermont, J., Robitaille, C., Auberson, Y. P., Bureau, G., and Cyr, M. (2011) Blockade of NMDA receptors 2A subunit in the dorsal striatum impairs the learning of a complex motor skill. *Behav. Neurosci.* **125,** 714–723 CrossRef Medline
42. Costa, R. M., Cohen, D., and Nicolelis, M. A. (2004) Differential corticostriatal plasticity during fast and slow motor skill learning in mice. *Curr. Biol.* **14,** 1124–1134 CrossRef Medline
43. Lewis, S. J., Dove, A., Robbins, T. W., Barker, R. A., and Owen, A. M. (2004) Striatal contributions to working memory: a functional magnetic resonance imaging study in humans. *Eur. J. Neurosci.* **19,** 755–760 CrossRef Medline
44. Reynolds, J. N., Hyland, B. I., and Wickens, J. R. (2001) A cellular mechanism of reward-related learning. *Nature* **413,** 67–70 CrossRef Medline
45. Charpier, S., Mahon, S., and Deniau, J. M. (1999) *In vivo* induction of striatal long-term potentiation by low-frequency stimulation of the cerebral cortex. *Neuroscience* **91,** 1209–1222 CrossRef Medline
46. Larson, J., and Munkácsy, E. (2015) Theta-burst LTP. *Brain Res.* **1621,** 38–50 CrossRef Medline
47. Eroglu, C., Allen, N. J., Susman, M. W., O'Rourke, N. A., Park, C. Y., Ozkan, E., Chakraborty, C., Mulinyawe, S. B., Annis, D. S., Huberman, A. D., Green, E. M., Lawler, J., Dolmetsch, R., Garcia, K. C., Smith, S. J., *et al.* (2009) Gabapentin receptor α2δ-1 is a neuronal thrombospondin receptor responsible for excitatory CNS synaptogenesis. *Cell* **139,** 380–392 CrossRef Medline
48. Lana, B., Page, K. M., Kadurin, I., Ho, S., Nieto-Rostro, M., and Dolphin, A. C. (2016) Thrombospondin-4 reduces binding affinity of [^{3}H]gabapentin to calcium-channel α2δ-1-subunit but does not interact with α2δ-1 on the cell-surface when co-expressed. *Sci. Rep.* **6,** 24531 CrossRef Medline
49. Zhang, F. X., Gadotti, V. M., Souza, I. A., Chen, L., and Zamponi, G. W. (2018) BK potassium channels suppress Cavα2δ subunit function to reduce inflammatory and neuropathic pain. *Cell Reports* **22,** 1956–1964 CrossRef Medline
50. Ma, H., Chen, S. R., Chen, H., Li, L., Li, D. P., Zhou, J. J., and Pan, H. L. (2018) α2δ-1 is essential for sympathetic output and NMDA receptor activity potentiated by angiotensin II in the hypothalamus. *J. Neurosci.* **38,** 6388–6398 CrossRef Medline
51. Ma, H., Chen, S. R., Chen, H., Zhou, J. J., Li, D. P., and Pan, H. L. (2018) α2δ-1 couples to NMDA receptors in the hypothalamus to sustain sympathetic vasomotor activity in hypertension. *J. Physiol.* **596,** 4269–4283 CrossRef Medline
52. Harris, K. M., Fiala, J. C., and Ostroff, L. (2003) Structural changes at dendritic spine synapses during long-term potentiation. *Philos. Trans. R Soc. Lond. B Biol. Sci.* **358,** 745–748 CrossRef Medline
53. Segal, M. (2005) Dendritic spines and long-term plasticity. *Nat. Rev. Neurosci.* **6,** 277–284 CrossRef Medline
54. Bliss, T. V., and Collingridge, G. L. (2013) Expression of NMDA receptor-dependent LTP in the hippocampus: bridging the divide. *Mol. Brain* **6,** 5 CrossRef Medline
55. Moussa, R., Poucet, B., Amalric, M., and Sargolini, F. (2011) Contributions of dorsal striatal subregions to spatial alternation behavior. *Learn. Mem.* **18,** 444–451 CrossRef Medline
56. Packard, M. G., and Teather, L. A. (1997) Double dissociation of hippocampal and dorsal-striatal memory systems by posttraining intracerebral injections of 2-amino-5-phosphonopentanoic acid. *Behav. Neurosci.* **111,** 543–551 CrossRef Medline
57. Yin, H. H., Mulcare, S. P., Hilário, M. R., Clouse, E., Holloway, T., Davis, M. I., Hansson, A. C., Lovinger, D. M., and Costa, R. M. (2009) Dynamic reorganization of striatal circuits during the acquisition and consolidation of a skill. *Nat. Neurosci.* **12,** 333–341 CrossRef Medline
58. Zhou, J. J., Yuan, F., Zhang, Y., and Li, D. P. (2015) Upregulation of orexin receptor in paraventricular nucleus promotes sympathetic outflow in obese Zucker rats. *Neuropharmacology* **99,** 481–490 CrossRef Medline
59. Friend, D. M., Devarakonda, K., O'Neal, T. J., Skirzewski, M., Papazoglou, I., Kaplan, A. R., Liow, J. S., Guo, J., Rane, S. G., Rubinstein, M., Alvarez, V. A., Hall, K. D., and Kravitz, A. V. (2017) Basal ganglia dysfunction contributes to physical inactivity in obesity. *Cell Metab.* **25,** 312–321 CrossRef Medline
60. Seibenhener, M. L., and Wooten, M. C. (2015) Use of the open field maze to measure locomotor and anxiety-like behavior in mice. *J. Vis. Exp.* **96,** 52434 CrossRef Medline
61. Patel, T. P., Gullotti, D. M., Hernandez, P., O'Brien, W. T., Capehart, B. P., Morrison, B., 3rd, Bass, C., Eberwine, J. E., Abel, T., and Meaney, D. F. (2014) An open-source toolbox for automated phenotyping of mice in behavioral tasks. *Front. Behav. Neurosci.* **8,** 349 Medline
62. Takao, K., Toyama, K., Nakanishi, K., Hattori, S., Takamura, H., Takeda, M., Miyakawa, T., and Hashimoto, R. (2008) Impaired long-term memory retention and working memory in sdy mutant mice with a deletion in Dtnbp1, a susceptibility gene for schizophrenia. *Mol. Brain* **1,** 11 CrossRef Medline